Islamic Azad University

Journal of
Optoelectronical Nanostructures

Summer 2024 / Vol. 9, No. 3

Research Paper

Terahertz Resonance Fluorescence of a Spherical Gaussian Quantum Dot

Behrooz Vaseghi[*,1], Ghasem Rezaei[1], Nasim Mohammadi[1], Shakiba Mardani[1]

[1]Department of Physics, College of Sciences, Yasouj University, Yasouj, Iran

Received: 12 Feb. 2024
Revised: 24 Mar. 2024
Accepted: 1 Jun. 2024
Published: 15 Sep. 2024

Keywords:
Resonance Fluoresce
Spherical Quantum Dot
Gaussian Confinement
Correlation Function
External Factors

Abstract:

Resonance fluorescence and related correlation functions of a spherical quantum dot with Gaussian confinement potential and doped hydrogen like impurity is studied. Similar to atomic systems we can see the resonance fluorescence with different photon statistics in the system. The results indicate that the physical parameters of the quantum dot significantly influence both the resonance spectrum and correlation functions.
The possibility of controlling the fluorescence phenomena via external parameters and dot engineering is an important result of the current study.

Citation: B.Vaseghi, G. Rezaei, N. Mohammadi, Sh. Mardani. Terahertz Resonance Fluorecence of a Spherical Gaissian Quantum Dot. **Journal of Optoelectronical Nanostructures. 2024; 9 (3): 19-32**
DOI: 10.30495/JOPN.2024.33226.1313

***Corresponding author: B. Vaseghi**
Address: Department of Physics, College of Sciences, Yasouj University, Yasouj, Iran
Tell: 00987431004160 **Email:** vaseghi@yu.ac.ir

1. INTRODUCTION

Resonant fluorescent (RF) is the scattering of an electromagnetic wave (EMW) from a free atom irradiated with a near-resonant field [1-3]. Three peaks appear in the emission spectrum known as Mollow triplets, first predicted by Mollow in 1969 [4-6]. This phenomena is one of the basic topics of quantum optics which is investigated theoretically and experimentally [7-12].

When a quantum emitter reaches plasmonic resonance conditions, the decay rate and near-field fields increase. This variation can change the populations of states and control the fluorescent spectrum of molecules and QDs [13, 15].

Quantum dots (QDs) attract much interest recently because they can be used to implement optical emitters and devices. Understanding the electronic states of QDs is r applications in electronics and optoelectronics [16-18]. ct of quantum confinement on the electronic states in QDs. K.p theory, pseudopotential (EP), single electron and other models have been studied widely to calculate physical properties of such systems [19-25].

In a quantum dot, a ladder of electronic energy levels emerges, leading to multiple anti-crossings as a result of the electrical Stark shift. Therefore, it is imperative to consider more than two electronic levels when identifying the accurate energy states in both experimental and theoretical measurements.

Here we have studied RF of a spherical Gaussian quantum dot (SGQD) and investigate the effects of dot properties and external electric field on the resonance fluorescence spectrum (RFS) and corresponding wave function. Using intersubband transition rather than bands transitions gives resonant peaks in the terahertz region of EMW radiation. Results show that dot parameters and external fields have considerable effects on RF and photon distributions.

2. RESONANCE FLUORESCENCE THEORY

When a quantum mechanical system interacts with a quantized electromagnetic (EM) field, its Hamiltonian can be expressed as follows under the rotating wave approximation:

$$H = \hbar\omega_a |a\rangle\langle a| + \hbar\omega_b |b\rangle\langle b| + \sum_{k,\lambda} \hbar\omega_k a^+_{k,\lambda} a_{k,\lambda} + \hbar \sum g_{k,\lambda} (\sigma_{ab} a_{k,\lambda} e^{i\vec{k}.\vec{r}_0} + \sigma_{ba} a^+_{k,\lambda} e^{-i\vec{k}.\vec{r}_0}) \quad (1)$$

Here two energy levels $|a\rangle$ and $|b\rangle$ with frequencies ω_a and ω_b, being the lower and upper energy states of the system, respectively (see Fig.1).

Additionally, $a_{k,\lambda}(t)(a^{+}_{k,\lambda}(t))$ is the annihilation (creation) operator for the k-th EM mode with frequency ω_k and polarization λ, $g_{k,\lambda}$ is the coupling constant between the k-th EM mode and the quantum transition $|a\rangle \leftrightarrow |b\rangle$.

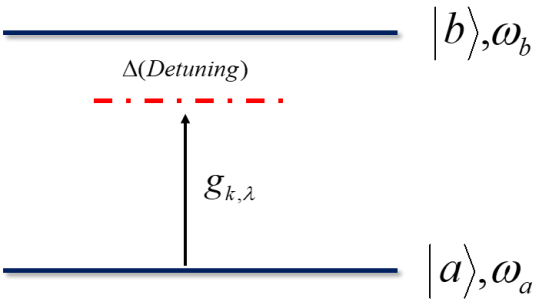

Fig.1 Schematic of a two-level atom

By using the slowly varying operators along with Heisenberg equation of motion, we can simultaneously determine the values of $a_{k,\lambda}(t)(a^{+}_{k,\lambda}(t))$ and $\sigma_{-}(t)(\sigma_{+}(t))$, Hamiltonian from Eq. (1). By inserting these operators into the quantized electric field operator, we can obtain

$$\vec{E}(\vec{r},t)=\sum_{k}\hat{e}_k\varepsilon_k a_k e^{-i\nu_k t+i\vec{k}.\vec{r}}+H.c. \tag{2}$$

and the following equation for emitted field, $E(\vec{r},t)$, in the Weisskopf-Wigner approximation

$$\vec{E}^{+}(\vec{r},t)=\frac{\omega^2\wp\sin\eta}{4\pi\varepsilon_0 c^2|\vec{r}-\vec{r}_0|}\hat{x}\sigma_{-}\left(t-\frac{|\vec{r}-\vec{r}_0|}{C}\right) \tag{3}$$

In the equations above $\varepsilon_k=(\hbar\nu_k/2\varepsilon_0 V)^{1/2}$, $\hbar\omega=E_b-E_a$ and $\wp$ is the electric dipole with angle η with the z-axis. In addition ε_0, is the vacuum

permittivity, and c is the speed of light. The power spectrum of the emission light in steady-state regime can be obtained by performing a Fourier transformation on the correlation function, $\left\langle E^{(-)}(r,t)E^{(+)}(r,t+\tau)\right\rangle$, when $t\to\infty$. Therefore, the power spectrum of the emission light in the far-field zone becomes

$$S(\vec{r},\omega_s)=\frac{1}{\pi}\mathrm{Re}\int_0^\infty d\tau\left\langle \vec{E}^{-}(\vec{r},t)\vec{E}^{|+}(\vec{r},t+\tau)\right\rangle e^{-i\omega_s\tau} \tag{4}$$

Based on the above equation RFS is [26]

$$S(\vec{r},\omega_0)=\frac{I_0(\vec{r})}{4\pi}\left(\frac{\Omega_R^2}{\Gamma^2+2\Omega_R^2}\right)$$
$$\times\left[\frac{4\pi\Gamma^2}{\Gamma^2+2\Omega_R^2}\delta(\omega-\omega_0)\right.$$
$$\left.+\frac{\Gamma}{(\omega-\omega_0)^2+(\Gamma/2)^2}+\frac{\alpha_+}{(\omega+\mu-\omega_0)^2+(3\Gamma/4)^2}+\frac{\alpha_-}{(\omega-\mu-\omega_0)^2+(3\Gamma/4)^2}\right] \tag{5}$$

and second order correlation function

$$G2(\tau)=1-(\cos\mu\tau+\frac{3\Gamma}{4\mu}\sin\mu\tau)\,e^{-3\Gamma\tau/4} \tag{6}$$

Where in the above equations

$$\alpha_\pm=\frac{3\Gamma}{4}P\pm(\omega\pm\mu-\omega_0)Q \tag{7}$$

$$P=\frac{2\Omega_R^2-\Gamma^2}{2\Omega_R^2+\Gamma^2}$$
$$Q=\frac{\Gamma}{4\mu}\frac{10\Omega_R^2-\Gamma^2}{2\Omega_R^2+\Gamma^2} \tag{8}$$

$$\mu=\left(\Omega_R^2-\frac{\Gamma^2}{16}\right)^{1/2} \tag{9}$$

Furthermore, Fermi's golden rule describes the absorption or emission of light by the charge carriers. This process involves a transition from the

initial energy state $|\psi_a\rangle$ to the final energy state $|\psi_b\rangle$, which is quantified by a transition rate, Γ.

$$\Gamma = \frac{1}{\tau_i} = \frac{2\pi}{\hbar}\sum_f \left|\langle \Psi_a | \frac{e}{m^*}\vec{A}.\vec{P}|\Psi_b\rangle\right|^2 \delta(E_a - E_b \mp \hbar\omega) \quad (10)$$

The vector potential of the drive radiation is represented by $\vec{A}$, and the momentum is represented by $\vec{P}$. The energies of the initial and final states are denoted as E_a and E_b. In a QD, the lifetime for inter-subband radiative emission is determined by summing Eq. (10) over all photon modes

$$\Gamma = \frac{1}{\tau_i} = \frac{1}{4\pi \in}\frac{4n\omega^3}{3\hbar c^3 \varepsilon}\frac{2\pi}{\hbar}\left|\langle \Psi_a | e\vec{r}.\vec{E}|\Psi_b\rangle\right|^2 \quad (11)$$

And the Rabi frequency is

$$\Omega_R = \frac{1}{\hbar}\left|\langle \Psi_a | e\vec{r}.\vec{E}|\Psi_b\rangle\right| \quad (12)$$

here $\in$ and n represent the permittivity and refractive index of the medium, while ε denotes the amplitude of the EM field.

3. MODEL OF THE QUANTUM DOT

The Hamiltonian governs the system of an off-center hydrogenic impurity in a SGQD, in the frame of the effective-mass approximation and with effective Rydberg units, under an applied external electric field, is as follows:

$$H = \frac{-\hbar^2}{2m^*}\nabla^2 - \frac{e^2}{\varepsilon|r-D|} + eFr\cos\theta + V(r) \quad (13)$$

The dielectric constant, ε, effective mass, m^*, position vector of the electron (impurity) from the center of the dot *r(D)*, electric field strength, *F*, and tilt angle to the z-axis, θ, all play a role in the representation of the Hamiltonian with a Gaussian confining potential as [27]

$$V(r) = -V_0 e^{-\frac{r^2}{R^2}} \quad (14)$$

In this equation, the depth of the potential well is represented by "$V_0 > 0$" and the dot radius is denoted by "R". To determine the energy eigenvalues and eigenfunctions of the SGQD, we have diagonalized the

total Hamiltonian of the system within the spanned model space. This is done by writing the total wave function as

$$\Phi_m = \sum_i c_i \psi_i(r) \tag{15}$$

Where

$$\psi_i(r) = R_{n_i l_i}(r) Y_{l_i m_i}(\theta, \varphi) \tag{16}$$

with the eigenvalues

$$E_i^{(0)} = (2n_i + l_i + \frac{3}{2})\hbar\omega_0 \tag{17}$$

and (n_i, l_i, m_i) refers to the magnetic and orbital quantum numbers. Considering that the impurity ion is located on the z-axis, without any loss of generality, one can expand the Coulomb interaction term in the Hamiltonian as:

$$\frac{1}{|r-D|} = \sum_{l=0}^{\infty} \frac{r_<^l}{r_>^{l+1}} P_l(\cos\theta) \tag{18}$$

Where $r_> = \max(r, D)$ and $r_< = \min(r, D)$. The elements of the total Hamiltonian matrix, *H*, are given by

$$\langle \Phi_m | H | \Phi_m \rangle = \sum_{i,j} \left\{ \left[2n_i + l_i + \frac{3}{2} \right] \hbar\omega\delta_{ij} + V_{ij} \right\} \tag{19}$$

with

$$\begin{aligned} V_{ij} = & \int_0^{\infty} R_{n_i l_i}(r) \left[V(r) - \frac{1}{2} m^* \omega^2 r^2 \right] R_{n_i l_i} r^2 dr \\ & - \int_0^{2\pi} d\Omega \int_0^{\infty} \psi_i^*(r) \left[\frac{e^2}{\varepsilon} \sum_{l=0}^{\infty} \frac{r_<^l}{r_>^{l+1}} P_l(\cos\theta) - eFr\cos\theta \right] \psi_i(r) r^2 dr \end{aligned} \tag{20}$$

4. RESULTS AND DISCUSSIONS

Resonance fluorescence and correlation function of a SGQD under the influence of external electric field and with off-center impurity is investigated in this paper. The main goal here is to investigate the possibility of its occurrence in the studied system and the effect of physical parameters on them. To calculate RFS and G2, using relations 11 and 12, the transition rate has been calculated and used. Since other scattering processes are not considered, their effect is entered

as an adjustable parameter. The parameters used in the calculations are: $\epsilon = 13.2, n = 3.2, m* = 0.067m$(m is the free electron mass).
In Figs. 2-7 RFS and related correlation function for different parameters of the system are calculated and plotted. In all cases it is seen that the RF occurs in the terahertz region of electromagnetic wave with different correlation function. In all figures, the rivalry between the normalized decay rate, Γ, and Rabi frequency, Ω_R, leads to different behaviors of RFS and G2 as the electronic structure of the system changes.
In Figs.2, 3 RFS and G2 are presented as a function photon energies and time for different values of impurity positions. It is clear that the position of hydrogenic impurities has a noticeable impact on S and G2. As the impurity position increases, the transition dipole moments decrease and the energy difference between subbands increases. As the D fluorescence increases, the linewidth decreases and two extra peaks are observed in the RFS. In addition, G2 becomes greater than 1, indicating photon antibunching, and a Poissonian distribution is observed for all D values.
Figs. 4,5 display RF and correlation function for different electric field strengths. Since electric field breaks symmetries thus energy difference between states increases and thus wave function overlap reduces as F enhances. This causes transition dipole moment decreases as F increases. Decrement of wave function overlap reduces transition dipole moments and thus different RF appear in the spectrum. With increasing F resonance sidebands become weaker and fluctuation in the photon distribution reduces. The effects of an electric field on the electronic structure are weak. Therefore, different values of F do not have a significant impact on the positions of the peaks and the linewidth of the RFS.**
To study the effects of confinement potential on the resonance fluorescent of the system in Figs. 6, 7 S and G2 are presented for different values of V_0. Because of the great reduction of dipole moments and energy different augments as V_0 increases thus, confining potential has considerable influence on the RFS and photon statistics of the system. It is evident that as V_0 decreases, the peaks of RFS decrease, the sidebands disappear, and photon antibunching occurs with a short lifetime.

The results presented here suggest that it is possible to control the fluorescence properties of nanostructures, particularly Gaussian quantum

dots, by adjusting external parameters. This could make the dots suitable for use in THz emitters.

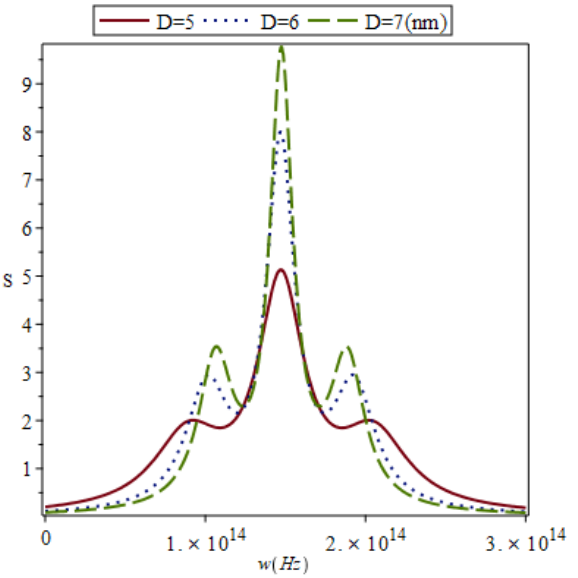

Fig.2 Resonance fluorescent spectrum as a function of photon frequency at different impurity positions.

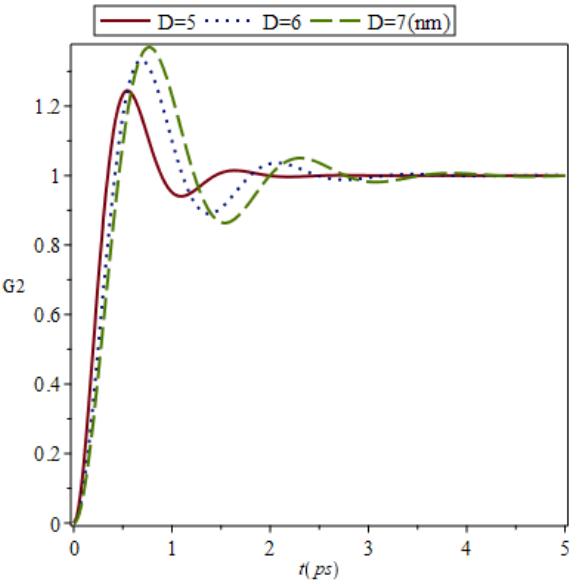

Fig.3 Second order correlation function as a function of delay time at different impurity positions.

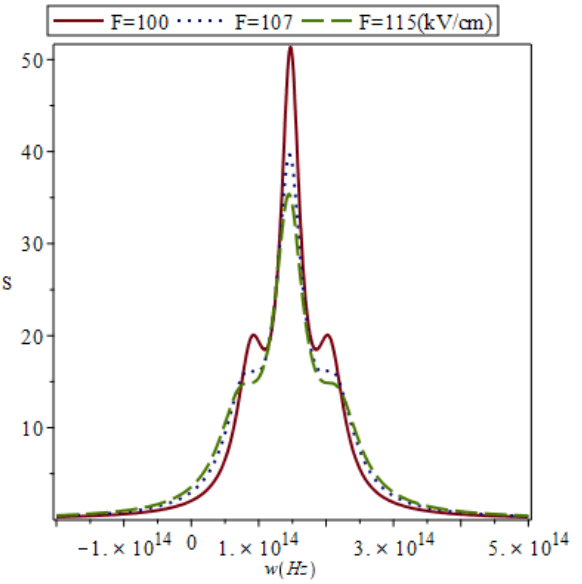

Fig.4 Resonance fluorescent spectrum as a function of photon frequency at different electric field strengths.

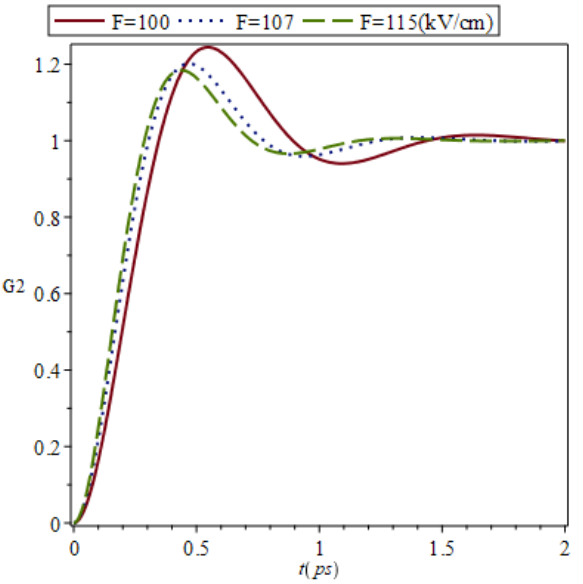

Fig. 5 Second order correlation function as a function of delay time at different electric field strengths.

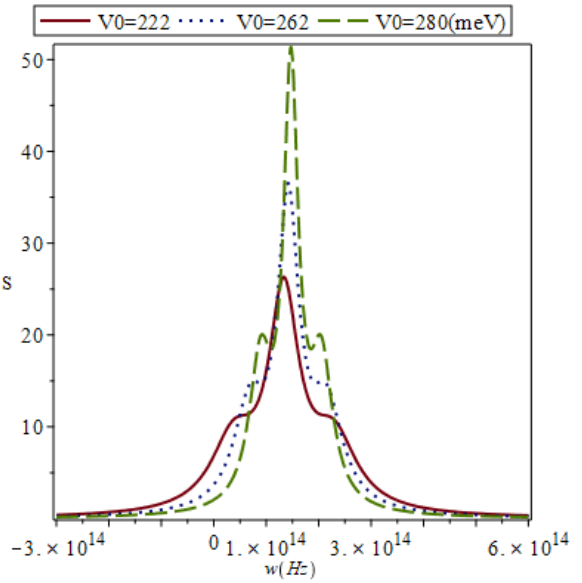

Fig.6 Resonance fluorescent spectrum as a function of photon frequency at different confining potentials.

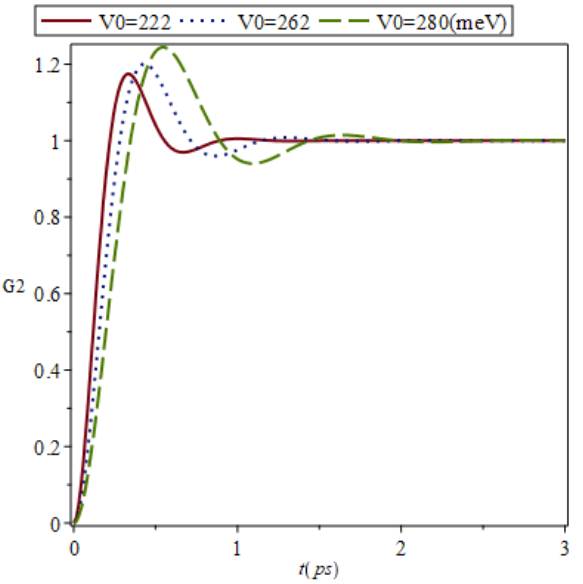

Fig.7

REFERENCES

[1] A. Gombkötö, A. Czirják, S. Varró, P. Földi, Quantum-optical model for the dynamics of high-order-harmonic generation, Phys. Rev. A 94 (2016) 013853. Available: https://doi.org/10.1103/PhysRevA.94.013853.

[2] L. Mandel, Squeezed States and Sub-Poissonian Photon Statistics, Phys. Rev. Lett. 49 (1982) 136. Available: https://doi.org/10.1103/PhysRevLett.49.136.

[3] P. Grangier, et. al., Observation of Photon Antibunching in Phase-Matched Multiatom Resonance Fluorescence, Phys. Rev. Lett. 57 (1986) 687. Available: https://doi.org/10.1103/PhysRevLett.57.687.

[4] B. R. Mollow, Power Spectrum of Light Scattered by Two-Level Systems, Phys. Rev. 188 (1969) 11969. Available: https://doi.org/10.1103/PhysRev.188.1969.

[5] F. Wu, et al., Investigation of the Spectrum of Resonance Fluorescence Induced by a Monochromatic Field, Phys. Rev. Lett. 35 (1975) 1426. Available: https://doi.org/10.1103/PhysRevLett.35.1426.

[6] C. H. R. Ooi, E. A. Sete, W. M. Liu, Quantum dynamics and spectra of vibrational Raman-resonance fluorescence in a two-mode cavity, Phys. Rev. A 92 (2015) 063847. Available: https://doi.org/10.1103/PhysRevA.92.063847.

[7] W. Vogel, D.G. Welsch, Quantum Optics, WILEY-VCH, Germany, 2006.

[8] M.O. Scully, S.M. Zubairy, Quantum Optics, Cambridge University Press, Cambridge, 2008.

[9] S. Wen, R. Zhang, S. Hu, L. Zhang, L. Liu, Improved fluorescence properties of core–sheath electrospun nanofibers sensitized by silver nanoparticles, Opt. Mater. 47 (2015) 263-269. Available: https://doi.org/10.1016/j.optmat.2015.05.038.

[10] F. Carreno, S. M. Razavi, M. A. Anton, Resonance fluorescence and phase-dependent spectra of a singly charged n-doped quantum dot in the Voigt geometry, Phys. Rev. B 95 (2017) 195310. Available: https://doi.org/10.1103/PhysRevB.95.195310.

[12] J. Enders, et.al., Nuclear resonance fluorescence experiments on ^{204,206,207,208}Pb up to 6.75 MeV, Nuclear Physics A 724 (2003) 243–273. Available: doi:10.1016/S0375-9474(03)01554-9.

[13] E. Scholl, et. al., Resonance Fluorescence of GaAs Quantum Dots with Near-Unity Photon Indistinguishability, Nano Lett. 19 (2019) 2404–2410. Available: https://doi.org/10.1021/acs.nanolett.8b05132; S. M. Barnett, et. Al., Decay of excited atoms in absorbing dielectrics, J. Phys. B 29 (1996) 3763. Available: DOI 10.1088/0953-4075/29/16/019.

[14] J. R. Lakowics, Plasmonics in Biology and Plasmon-Controlled Fluorescence, Plasmonics 1(2006) 5-33. Available: doi: 10.1007/s11468-005-9002-3.

[15] D. Wigger, M. Weiß, M. Lienhart, K. Müller, J. J. Finley, T. Kuhn, H. J. Krenner, P. Machnikowski, Resonance-fluorescence spectral dynamics of an acoustically modulated quantum dot, Phys. Rev. Research 3 (2021) 033197. Available: https://doi.org/10.1103/PhysRevResearch.3.033197.

[16] S. Kahmann, A. Shulga, M. A. Loi, Quantum Dot Light-Emitting Transistors—Powerful Research Tools and Their Future Applications, Advanced Functional Materials 30 (2020) 1904174. Available: https://doi.org/10.1002/adfm.201904174.

[17] E. Parto, G. Rezaei, A. Mohammadi Eslami, T. Jalali, Finite difference time domain simulation of arbitrary shapes quantum dots, Eur. Phys. J. B 92 (2019) 246. Available: https://doi.org/10.1140/epjb/e2019-100410-9.

[18] B. Vaseghi, M. Sadri, G. Rezaei, A. Gharaati, Optical rectification and third harmonic generation of spherical quantum dots: Controlling via external factors, Physica B 457 (2015) 212-217. Available: https://doi.org/10.1016/j.physb.2014.10.020.

[19] C. H. H. Schulte, J. Hansom, A. E. Jones, C. Matthiesen, C. Le Gall, M. Atatüre, Quadrature squeezed photons from a two-level system, Nature 525 (2015) 222-225. Available: https://doi.org/10.1038/nature14868.

[20] T. Takagahara, K. Takeda, Theory of the quantum confinement effect on excitons in quantum dots of indirect-gap materials, Phys. Rev. B 46 (1992) 15578. Available: https://doi.org/10.1103/PhysRevB.46.15578.

[21] G. Singh Selopal, H. Zhao, Z. M. Wang, F. Rosei, Core/Shell Quantum Dots Solar Cells, Advanced Functional Materials 30 (2020) 1908762. Available: https://doi.org/10.1002/adfm.201908762.

[22] H. N. Gopalakrishna, R. Baruah, C. Hünecke, V. Korolev, M. Thümmler, A. Croy, M. Richter, F. Yahyaei, R. Hollinger, V. Shumakova, I. Uschmann, H. Marschner, M. Zürch, C. Reichardt, A. Undisz, J. Dellith, A. Pugžlys, A. Baltuška, C. Spielmann, U. Peschel, S. Gräfe, M. Wächtler, and D. Kartashov, Tracing spatial confinement in semiconductor quantum dots by high-order harmonic generation, Phys. Rev. Research 5 (2023) 013128. Available: https://doi.org/10.1103/PhysRevResearch.5.013128.

[23] L. A. Cipriano, G. Di Liberto, S. Tosoni, G. Pacchioni, Nanoscale 12 (2020) 17494-17501. Available: https://doi.org/10.1039/D0NR03577G.

[24] A. Jahanshir, Quanto-Relativistic Background of Strong Electron-Electron Interactions in Quantum Dots under the Magnetic Field JOPN 6 (2021) 1-24. Available: DOI: 10.30495/JOPN.2021.28742.1231

[25] H. Bahramiyan, S. Bagheri, Linear and nonlinear optical properties of a modified Gaussian quantum dot: pressure, temperature and impurity effect, JOPN 3 (2018) 79-100.

Available: https://jopn.marvdasht.iau.ir/article_3047_0a2d460925ad6686daf5ac62c9082227.pdf

[26] S. M. Razavi, B. Vaseghi, Terahertz resonance fluorescence and squeezing in quantum dots: Effects of external electric field and dimension, Optik 158 (2018) 460. Available: https://doi.org/10.1016/j.ijleo.2017.12.180.

[27] S. Taghipour, G. Rezaei, A. Gharaati Electromagnetically induced transparency in a spherical Gaussian quantum dot, Eur. Phys. J. B. 95 (2022) 141. Available: https://doi.org/10.1140/epjb/s10051-022-00409-7.